HHS Public Access

Author manuscript

Brain Behav Immun. Author manuscript; available in PMC 2024 November 01.

Published in final edited form as:

Brain Behav Immun. 2023 November ; 114: 311–324. doi:10.1016/j.bbi.2023.08.020.

Acetate supplementation rescues social deficits and alters transcriptional regulation in prefrontal cortex of *Shank3* deficient mice

Aya Osman[1,2,3], **Nicholas L. Mervosh**[1,2], **Ana N. Strat**[3], **Tanner J. Euston**[1], **Gillian Zipursky**[1], **Rebecca M. Pollak**[1,2], **Katherine R. Meckel**[1,3], **Scott R. Tyler**[4], **Kenny L. Chan**[3], **Ariela Buxbaum Grice**[1,2,4], **Elodie Drapeau**[1,2], **Lev Litichevskiy**[5], **Jasleen Gill**[6], **Sharon M. Zeldin**[1], **Christoph A. Thaiss**[6,7,8], **Joseph. D. Buxbaum**[1,2,3,4], **Michael S. Breen**[1,2,4], **Drew D. Kiraly**[1,2,3,9,10,*]

[1]Department of Psychiatry, Icahn School of Medicine at Mount Sinai, New York, New York 10029, United States

[2]Seaver Autism Center for Research and Treatment, Icahn School of Medicine at Mount Sinai, New York, New York 10029, United States

[3]Nash Family Department of Neuroscience, Icahn School of Medicine at Mount Sinai, New York, New York 10029, United States

[4]Department of Genetics and Genomic Sciences, Icahn School of Medicine at Mount Sinai, New York, New York 10029, United States

[5]Department of Biostatistics, Epidemiology and Informatics, Perelman School of Medicine, University of Pennsylvania, Philadelphia, PA

[6]Department of Microbiology, Perelman School of Medicine, University of Pennsylvania, Philadelphia, PA, USA

[7]Institute for Immunology, Perelman School of Medicine, University of Pennsylvania, Philadelphia, PA, USA

[8]Institute for Obesity, Diabetes and Metabolism, Perelman School of Medicine, University of Pennsylvania, Philadelphia, PA, USA

[9]Department of Physiology & Pharmacology, Wake Forest University School of Medicine, Atrium Wake Forest Baptist Health, Winston-Salem, North Carolina 27101, United States

[*]Corresponding author: Drew D. Kiraly, 115 South Chestnut Street, Winston-Salem, North Carolina, 27101. dkiraly@wakehealth.edu. Twitter: @Kiralylab.

Author Contributions

A.O., N.L.M., A.N.S, T.J.E, G.Z., K.R.M., L.L., C.A.T. & D.D.K. performed experiments; A.O., S.R.T., K.L.C, A.B.G., E.D., L.L., J.G., C.A.T., M.S.B., & D.D.K analyzed data; A.O., E.D., J.D.B., M.S.B., & D.D.K contributed to experimental design; J.D.B. generated the mouse line; A.O. & D.D.K. wrote the manuscript; All authors contributed critical edits and feedback on the final manuscript draft.

Disclosures

The authors declare no competing interests in this work.

[10]Department of Psychiatry, Wake Forest University School of Medicine, Atrium Wake Forest Baptist Health, Winston-Salem, North Carolina 27101, United States

Abstract

Background—The pathophysiology of autism spectrum disorder (ASD) involves genetic and environmental factors. Mounting evidence demonstrates a role for the gut microbiome in ASD, with signaling via short-chain fatty acids (SCFA) as one mechanism. Here, we utilize mice carrying deletion to exons 4–22 of *Shank3* (*Shank3*^{KO}) to model gene by microbiome interactions in ASD. We identify SCFA acetate as a mediator of gut-brain interactions and show acetate supplementation reverses social deficits concomitant with alterations to prefrontal cortex (mPFC) transcriptional regulation independent of microbiome status.

Methods—*Shank3*^{KO} and wild-type (Wt) littermates were divided into control, Abx, Acetate and Abx+Acetate groups upon weaning. After six weeks, animals underwent behavioral testing. Molecular analysis including 16S and metagenomic sequencing, metabolomic and transcriptional profiling were conducted. Additionally, targeted serum metabolomic data from Phelan McDermid Syndrome (PMS) patients (who are heterozygous for the *Shank3* gene) were leveraged to assess levels of SCFA's relative to ASD clinical measures.

Results—*Shank3*^{KO} mice were found to display social deficits, dysregulated gut microbiome and decreased cecal levels of acetate – effects exacerbated by Abx treatment. RNA-sequencing of mPFC showed unique gene expression signature induced by microbiome depletion in the *Shank3*^{KO} mice. Oral treatment with acetate reverses social deficits and results in marked changes in gene expression enriched for synaptic signaling, pathways among others, even in Abx treated mice. Clinical data showed sex specific correlations between levels of acetate and hyperactivity scores.

Conclusion—These results suggest a key role for the gut microbiome and the neuroactive metabolite acetate in regulating ASD-like behaviors.

(1) Introduction

Autism spectrum disorder (ASD) is a potentially serious neurodevelopmental disorder characterized by deficits in social function and stereotyped and repetitive behaviors[1]. The pathophysiology of ASD is complex and involves a combination of genetic and environmental risk factors. While significant strides have been made in determining the genetic basis of ASD with over 100 high risk gene loci identified (e.g. *Fmr1*, *Shank3*)[2–4], environmental contributions to ASD remain less well defined. There is a growing body of evidence suggesting the resident bacteria of the gastrointestinal tract (GI), known as the gut microbiome play a key role in host brain development and behavior through a mechanism known as the gut-brain axis[5], which has been implicated in neurodevelopmental disorders.

Clinical data shows higher rates of co-occurring GI disturbances[4,6], as well as changes in microbiome composition[6–8] and metabolic profile[9,10] in patients with ASD compared to neurotypical controls. Moreover, early studies in mice lacking a microbiome (germ free) show marked deficits in social behaviors and brain region specific gene expression changes[11–13]. Additionally, mice who have had their microbiomes depleted with antibiotics

(Abx) show deficits in social behavior, cognitive flexibility, and multiple other ASD-like behaviors[7,18,19]. At a cellular and molecular level, disruption of the microbiome with prolonged Abx leads to changes in neuronal and glial structure, changes in cell firing patterns, and altered transcriptional and epigenetic signatures in in the brain[14–17]. Despite this accumulating evidence, the exact bacterial species and metabolites similarly altered across studies in ASD and the mechanisms by which gut bacteria influence the brain remain elusive.

The strongest literature suggests the production of neuroactive metabolites by the microbiome as a key gut-brain signaling mechanism[16,18,19]. Among the best studied metabolites in this gut-brain axis are the short-chain fatty acids (SCFA) which are produced in the process of bacterial fermentation of fiber and can cross the blood-brain barrier, influence chromatin structure and gene expression in behaviorally relevant ways[20,21].

While the literature demonstrating a gut-brain connection in ASD is robust and continues to grow, there are few studies specifically modeling gene by microbiome interactions. An attractive gene candidate for this line of research is the *Shank3* gene which encodes a synaptic scaffolding protein and is the causative gene underlying Phelan McDermid Syndrome (PMS). Importantly, patients with PMS manifest features of ASD with cognitive impairments and co-occurring gastrointestinal issues[4] suggesting a potential for a gut brain link. Indeed, studies found changes in the gut microbiome composition in relation to ASD-like phenotypes in mice and zebrafish lacking specific *Shank3* isoforms[22–24].

Here we utilize a mouse model with deletion of exons 4–22 of the *Shank3* gene resulting in lack of all functional isoforms of *Shank3* (*Shank3*^{KO})[25]. Using 16S and metagenomic sequencing, and targeted metabolomics we identify changes in microbiome form and function driven by *Shank3* genotype. Additionally, *Shank3*^{KO} mice are particularly sensitive to behavioral and metabolic effects of microbiome alterations. Using RNA-sequencing of the frontal cortex we identify a unique gene expression signature induced by microbiome depletion in the *Shank3*^{KO} mice. Oral treatment with the SCFA acetate was found to reverse social deficits and markedly altered cortical transcriptional regulation, even in mice lacking a microbiome. Finally, correlations between levels of acetate and ASD behavioral phenotypes in patients with PMS were identified. Taken together, our data build on existing work identifying important gene by microbiome interactions in ASD and provide a mechanism of this interaction via identification of a specific microbial metabolite.

(2) Materials and Methods

2.1 Mice

Both male and female mice wild-type (Wt) or homozygous (KO) for the *Shank3* gene were generated from heterozygous *Shank3* breeders on a C57BL/6J background[25]. Littermates were weaned at PND21, separated by sex and caged with 2–4 other littermates with a mixture of genotypes per cage to avoid cage effects on analysis. Food was available ad libitum throughout experiments, and drinking water was modified as described below. The colony room was maintained at constant temperature of 21°C and 55% humidity with a 12-hour light dark cycle (on 0700/off 1900). Animal procedures were approved by the

Institutional Animal Care and Use Committee of the Icahn School of Medicine at Mount Sinai.

2.2 Drink Solutions

For Experiment 1 (Fig.1), immediately after weaning (on ~PND21), mice were maintained on standard vivarium drinking water as control animals. For Experiment 2 (Fig.2 & 3), immediately after weaning mice were split into control (H_2O) or Abx treatment groups and for Experiment 3 (Fig.4,5 &6) mice were split into control (H_2O), Abx, Acetate, and Abx+Acetate (Ab/Ac) groups. In all three experiments, control mice were provided with standard vivarium drinking water. Abx mice received drinking water containing a non-absorbable antibiotic cocktail (Abx - Neomycin 2 mg/ml, Pimaricin 1.2 ug/ml, Vancomycin 0.2 g/ml, and Bacitracin 0.5 mg/ml)[16]. Acetate treatment groups received drinking water containing 100 mM Sodium Acetate (Sigma #S5636). Ab/Ac groups received Abx and Acetate at the described concentrations. Mice were maintained on treatments for the duration of the experiments. Bottle weights and body weights were collected from a subset of mice twice a week for the first two weeks of treatment then weekly afterwards.

2.3 Behavioral assessments

2.3.1 Three chambered Social Interaction Test—Sociability was assessed using the three chambered apparatus according to standard procedures[71]. The three chambers of the arena were designated using the Noldus software. Mice were first allowed to habituate to the middle chamber for 5 minutes, then habituate to the whole 3 chamber box without the empty wire cups for 10 minutes. The final stage consisted of placing an unfamiliar mouse under a wire cup in one chamber and an empty cup in another chamber. The amount of time test subjects spends in each chamber containing empty cup or unfamiliar mouse was automatically calculated using Noldus Ethovision-full details in Supplemental Methods.

2.3.2 Open field—For anxiety-like behavior, mice were placed in the center of an open field arena and allowed to move freely for 1 hour. The arena was virtually divided into central and peripheral regions using the Noldus software. The total distance travelled, as well as the total time spent in the center were calculated by video tracking (Noldus Ethovision)- full details in Supplemental Methods.

2.3.3 Elevated Zero Maze—To further assess anxiety-like behavior, mice were placed in the center of an open arm of an elevated zero maze (Maze Engineers) and allowed to move freely for 5 minutes. The arena was virtually divided into open and closed regions using the Noldus software. Mouse activity was recorded by video tracking (Noldus Ethovision). The duration and frequency of entries into the open arms were calculated- full details in Supplemental Methods.

2.3.4 Behavior Statistical Analysis—All behaviors were analyzed with two-way ANOVAs with Holm-Sidak post hoc tests as appropriate for 2×2 experiments, and as two-tailed T-tests for pairwise comparisons.

2.4 16s-Sequencing and Data Analysis

DNA from flash frozen cecal content was isolated using QiaAmp DNA stool kit (Qiagen) according to manufacturer instructions[17]. Data analysis was performed using QIIME v1.8.0[26] with standard settings. Full details in Supplemental Methods.

2.5 Shotgun Metagenomic Sequencing and Data Analysis

Bacterial genomic DNA was isolated from frozen cecal samples as described for 16S analysis and subjected to metagenomic sequencing. Metagenomic data were pre-processed using Sunbeam[27]. DIAMOND[28] was used to align reads to all prokaryotic protein sequences from KEGG[29]. For pathway analysis, KEGG Orthologs (KOs) with differential abundance between genotypes and treatment groups were identified using DESeq2[30]. Full details in Supplemental Methods.

2.6 Cecal Metabolomics

Levels of both SCFAs and amino acids were quantified from cecal content collected from test animals using a Water Acquity uPLC System with a Photodiode Array Detector using standard methods from the UPenn metabolomics centre-full details in Supplemental Methods.

2.7 RNA-Sequencing and Data Analysis

RNA isolation from mPFC, assessment of RNA integrity, Poly-A library preparation, and 2×150bp paired-end sequencing were performed according to standard procedures. For differential gene expression (DGE) analysis, aligned reads were subjected to voom normalization[31]. DGE signatures between samples were identified using moderated *t*-test in the LIMMA package[31]. The following covariates were included in the LIMMA model to adjust for their potential confounding influence on gene expression between group main effects: treatment group, sex and genotype. Additionally, a surrogate variable analysis was conducted which identified and regressed out 5 variables besides treatment, sex and genotype on DGE signatures[32]. Statistical significance threshold was set as a surrogate adjusted nominal *p*-value of < 0.01 to generate gene lists for functional characterization. Given the complexity of the experimental design (eight total groups), all pairwise comparisons shown were conducted to the ultimate control group (Wt-H_2O). Gene ontology enrichment analysis was performed using G:Profiler with default settings[33], and predicted transcriptional regulators were identified utilizing Enrichr software with the ENCODE and CHEA databases[33]. Additional details as per Supplemental Methods.

2.8 Mouse Serum Metabolomics and Data Analysis

Targeted SCFA and untargeted metabolomic analysis using liquid chromatography-mass spectrometry (LC/MS) was conducted on serum samples collected from test animals using chemical isotope labeling and pathway analysis as described previously[34]. Full details in Supplemental Methods.

2.9 Human Plasma Metabolomics and Statistical Analysis

We leveraged published plasma metabolomic profiles derived from 32 PMS probands and 28 controls (siblings n=27; parent n=1)[35]. A targeted panel of eight SCFA metabolites was generated. Data quality control was conducted as previously described[35]. A moderated t-test from LIMMA was used to assess the effect of categorical variables on SCFA levels. Correlative analysis was also conducted using LIMMA to assess the effect of quantitative variables on levels of SCFA's. Empirical Bays method was used to calculate moderated t and F statistics for both types of analysis. Adjusted p <0.05 was accepted as statistically significant. Full details in Supplemental Methods.

2.10 Figures

Graphs of all figures were created in Graphpad Prism and R. Experimental timelines were generated in BioRender with full permission to publish.

(3) Results

3.1 Deletion of the Shank3 Gene Results in a Dysregulated Gut Microbiome and Metabolic Output

To identify effects of *Shank3* gene deletion on microbiome composition and metabolic output, both 16S ribosomal and shotgun metagenomic sequencing was performed on cecal contents of untreated Wt and *Shank3*^{KO} mice in adulthood (~P60) (Fig. 1A-Experiment 1). To control for potential maternal and environmental confounds, analysis was performed on littermates caged according to sex, with each cage containing 2–5 mice of various genotypes. 16S-seq showed alpha diversity, which calculates the richness and evenness of diversity within samples[36], is significantly decreased in *Shank3*^{KO} mice when calculated by both the Simpson (Fig. 1B– p = 0.01) and Shannon (Fig. 1C– p = 0.03) diversity indices. Shifts in relative expression of bacterial phyla in the two genotypes are qualitatively presented (Fig. 1D). The most abundant bacterial phyla in the gut are the Bacteroidetes and Firmicutes, and their presence and relative abundance have been tied to health of the microbiome[37]. *Shank3*^{KO} exhibit a significant decrease in the Firmicutes phylum (Fig. 1E– p = 0.003) a trend toward an increase in Bacteroidetes phylum (Fig. 1F– p = 0.08) and a significant decrease in Firmicutes/Bacteroidetes ratio (Fig. 1G– p = 0.02). All statistical results are summarized in Table S1.

Next, examination of phylogeny within Firmicutes down to the species level showed class Bacilli, order Lactobacillales, family *Lactobacillaceae*, and genus *Lactobacillus* were significantly reduced in *Shank3*^{KO} (Fig. 1H- main effect of genotype $F_{(1,55)}$=196.4 p < 0.001 and main effect of taxonomical class $F_{(4,55)}$=7.990; p < 0.001; all significant by Holm-Sidak post-hoc testing p < 0.001). A list of changes at each taxonomical level is in Table S2. These microbial changes translated to an altered metagenomic profile characterized by increases in KEGG pathway relative counts corresponding to Fatty Acid degradation (Fig. 1I p = 0.02) and phenylalanine metabolism (Fig. 1J- p = 0.006). This is of note as both pathways are important in gut brain signaling[15]. A full list of metagenomic pathways altered by genotype can be found in Table S3.

Given the production of neuroactive metabolites is implicated in gut-brain signaling, targeted metabolomics analysis was performed on levels of SCFA and amino acids from cecal contents of Wt and *Shank3*^{KO} mice[38,39]. *Shank3*^{KO} have a specific significant decrease in acetate (Fig. 1K– main effect of genotype $F_{(1,33)}$=5.847 p = 0.0213). Genotype differences in several amino acids including essential amino acids leucine and phenylalanine are also present (Fig. 1L– main effect of genotype $F_{(1,46)}$=18.81 p < 0.0001). These results demonstrate *Shank3*^{KO} mice have marked disruptions of gut microbiome composition and function at baseline.

3.2 Microbiome depletion interacts with *Shank3* genotype to affect microbial, metabolic and behavioral phenotypes

To interrogate effect of microbiome composition in *Shank3* deficient mice, experiments using Abx induced microbiome depletion starting immediately after weaning (~P21) and continuing through adulthood (~P60) were conducted, with all behavioral assessments occurring at ~P60 (Fig. 2A - Experiment 2). By reducing microbiome bulk and diversity, interaction between *Shank3* genotype and microbiome status can be assessed. Abx treatment did not affect weight gain over time (Fig. 2B-main effect of time: $F_{(1.44, 24.40)}$ = 260.0 - p<0.0001) or levels of drinking (Fig. 2C- p = 0.35) and reduced microbial diversity as assessed by Shannon alpha diversity index (Fig. 2D-main effect of Abx - $F_{(1,16)}$ = 19.82; p=0.0004) and beta (Fig. 2E) diversity measures. Furthering our targeted metabolomics, levels of acetate are decreased by microbiome depletion and this effect is particularly pronounced in *Shank3*^{KO} mice (Fig. 2F-main effect of genotype: $F_{(1,17)}$ = 9.615; p=0.007 and main effect of Abx: $F_{(1,17)}$ = 12.67; p=0.002. Pairwise Holm-Sidak post-hoc results in Table S1).

To test how manipulations to microbiome would affect *Shank3*^{KO} behavioral phenotypes, control and Abx treated mice were assessed on a series of ASD relevant behavioral paradigms. On a three-chamber social interaction task, a strong group by social stimulus interaction was observed (Fig. 2G - $F_{(3,108)}$ = 6.35; p=0.0005), but no main effects of genotype or treatment. Wt mice form the expected preference for the social chamber (**2G-light blue**-p = 0.0046), however Wt-Abx mice did not express significant social preference (**2G-dark blue** - p = 0.4). *Shank3*^{KO}-H_2O mice showed no baseline social preference as expected (**2G-pink**- p = 0.4), and *Shank3*^{KO}-Abx mice showed a significant aversion for the socially paired chamber (**2G-red bars** – p = 0.01). Thus, demonstrating that both microbiome manipulation and *Shank3* deletion impair sociability, with stronger effects in microbiome depleted *Shank3*^{KO} mice.

Next, similarly treated Wt and KO mice were assessed for locomotor and anxiety-like behavior. On a 60-minute open field task, there was a marked effect of genotype on distance travelled (Fig. 2H $F_{(1,57)}$ = 11.15; p=0.0015) consistent with previous reports on this mouse line[33]. On this paradigm, there was no significant effect of time spent in the center (Fig. 2I-– All main effects and interactions p > 0.13) which is frequently used as a measure of anxiety-like behavior. Anxiety-like behavior was further assessed using an elevated zero maze, where there were no significant differences with genotype or treatment (Fig. 2J-All main effects and interactions p > 0.13). However, *Shank3*^{KO} mice did show a

modest increase in the number of total open arm entries (Fig. 2K-main effect of genotype $F_{(1,54} = 6.61$; p=0.13). Interestingly, Post hoc pairwise comparison showed only KO-H_2O mice displayed increased open arm entries compared to Wt-H_2O (Fig. 2K $p = 0.015$), but not KO-Abx mice– suggesting that Abx treatment may serve to moderate anxiety-like behavior as assessed by the elevated zero maze. Together, we find no consistent effect of *Shank3* deletion or microbiome depletion on anxiety like behavior, and genotype effects on locomotion when assessed over a longer period.

3.3 Microbiome depletion interacts with *Shank3* genotype to affect transcriptional regulation in medial prefrontal cortex.

Following behavioral testing, medial prefrontal cortex (mPFC) was dissected for full transcriptomic profiling (Fig. 2A). This brain region was selected as a critical mediator of social behaviors[40–42], is directly affected by *Shank3* deletions[43–45], and is affected by alterations in microbiome composition[18,46,47]. All pairwise comparisons made for this analysis were compared to the ultimate control group (Wt-H_2O) to enable assessment of how each manipulation (genotype, treatment or both) led to deviations in gene expression from this baseline. The Wt-Abx vs.Wt-H_2O comparison (Fig. 3A) which enables assessment of Abx effects on gene expression in Wt animals shows regulation of approximately 500 genes. With increases in pathways related to cellular structure and decreases in pathways related to synaptic function among others (Fig. 3B; Full DEG lists for Fig. 3 available in Table S4, and all significant GO pathways in Table S5). The KO-H_2O vs. Wt-H_2O comparison (Fig. 3C), which enables assessment of $Shank3^{KO}$ effects on gene expression, showed regulation of just over 300 genes. With notable decreases in pathways related to metabolism and DNA binding (Fig. 3D). Interestingly, the KO-Abx (demonstrated the most robust effects on social interaction) vs Wt-H_2O comparison, which enables assessment of both $Shank3^{KO}$ and Abx effects on gene expression, had the smallest number of differentially expressed genes at a total count of just over 200 genes (Fig. 3E). These genes were enriched for pathways related to cytosolic processes and anatomical processes (Fig. 3F).

When gene expression patterns between Wt-Abx and KO-Abx mice relative to Wt-H_2O were examined in more detail, little overlap was found (Fig. 3G) indicating the genes changed by Abx treatment relative to Wt control in each genotype are distinct. Gene ontology analysis of Abx-regulated genes in each genotype showed pathways for protein metabolism, binding, and cellular anatomy were more altered in Wt-Abx mice than in $Shank3^{KO}$-Abx mice (Fig. 3H). Similarly, Enrichr identified different predicted transcriptional regulators and epigenetic enzymes involved in the two Abx gene sets (Fig. 3I). Together, this suggests *Shank3* genotype significantly affects mPFC transcriptional response to microbiome depletion and provide evidence for the discrepant behavioral phenotypes observed.

3.4 Acetate Replenishment Rescues Social Deficits Caused by *Shank3* Gene Deletion Independent of Microbiome Status

Levels of acetate were regulated by *Shank3* genotype and microbiome depletion. Acetate inhibits histone deacetylases[48], alters brain gene expression and behavior[49], and plays a

role in regulating satiety mechanisms[50]. Given such evidence, manipulations to levels of acetate were performed in *Shank3*^{KO} mice followed by behavioral assessment to determine its mechanistic function. For these experiments, both Wt and KO mice were again put on control or Abx drink solutions as described above for Experiment 2, with additional groups treated with acetate or Ab/Ac added to assess effects of acetate independent of microbiome status (Fig. 4A - Experiment 3). All genotypes and treatment groups were behaviorally tested in parallel. For analysis of results, control water treated groups were directly compared to acetate groups to enable assessment of acetate supplementation without microbiome manipulation on behavior. Similarly, to determine the effect of acetate in reversing effects of microbiome depletion, Abx groups were directly compared to Ab/Ac groups.

Importantly, Acetate and Ab/Ac treatment did not affect body weight gain overtime (Supp Fig. 1A - Main effect of time: $F_{(1,29)} = 253.0$ - $p<0.0001$) or levels of drinking across the experiment (Supp Fig. 1B $p>0.05$). Interestingly, there is a significant treatment x genotype interaction on the Shannon index of alpha diversity (Fig. 4B Interaction $F_{(1,17)} = 8.927$ – $p=0.0083$). However, there were no main effects of acetate or genotype and individual post-hoc comparisons were not significant (Table S1).

In the three-chamber social interaction paradigm, treatment with Acetate resulted in a main effect of social stimulus (Fig. 4C - $F_{(1,66)} = 25.90$; $p < 0.0001$) and a borderline social stimulus by group interaction ($F_{(3,66)} = 2.18$; $p =0.09$). Planned pairwise Holm-Sidak post-hoc comparisons showed Wt-H_2O mice form a significant preference for the social stimulus (**4C** blue bars – $p = 0.0002$) which was not affected by acetate supplementation (**4C** green bars – $p = 0.006$). As with our previous experiments, KO-H_2O mice did not form a significant preference for the social stimulus (**4C** pink bars – $p = 0.87$). However, KO-Acetate mice showed a marked reversal of the *Shank3* genotype effect and exhibit a significant preference for the social chamber (**4C** purple bars – $p = 0.003$). On measures of locomotion, acetate treatment induced a significant genotype by treatment interaction during a 1-hour open field test (**4D** - interaction $F_{(1, 43)} = 4.113$ $p=0.0488$) where KO-Acetate mice no longer show the hypomobile phenotype seen in KO-H_2O mice (**4D** - $p = 0.0344$). While there were no significant effects of genotype or acetate treatment on time in the center of the open field (Fig. 4E- $p > 0.17$ for all), further assessment of anxiety-like behavior using the elevated zero maze, showed a modest genotype effect on time in the open arms (Fig. 4F- $F_{(1,59)} = 4.69$; $p =0.03$). Similarly, the frequency of open arm entries was increased by *Shank3*^{KO} status (Fig. 4G - $F_{(1,60)} = 8.70$; $p =0.0045$). Interestingly, post hoc pairwise comparison showed only KO-H_2O mice displayed increased open arm entries compared to Wt-H_2O (Fig. 4G $p = 0.0089$), but not KO-Acetate mice– suggesting that acetate treatment may serve to moderate this behavioral phenotype.

Next, the effects of acetate supplementation on the behavioral effects of microbiome depletion in Wt and *Shank3*^{KO} mice was assessed. As expected, treatment with acetate did not reverse Abx effects on microbiome diversity (Fig. 4H). In the three chambered social interaction task, there was a main effect of social stimulus (Fig. 4I - $F_{(1, 56)} = 7.598$ p=0.0079) and a social stimulus by group interaction ($F_{(3,56)} = 10.82$; $p <0.0001$). As seen in the initial cohort, Wt mice treated with Abx did not exhibit significant preference for the

social stimulus (**4I** blue bars – $p = 0.1$) and KO-Abx mice exhibited a significant aversion of the social chamber (**4I** red bars – $p = 0.004$). However, when mice were treated with Abx in combination with acetate, Abx induced social deficits were completely reversed in both Wt (**4I** green bars – $p < 0.0001$) and KO mice (**4I** purple bars – $p = 0.0005$).

In the open field task, Ab/Ac treatment did not obviate the genotype effect of decreased locomotion at one hour (Fig. 4J- $F_{(1,55)} = 9.51$; $p = 0.003$), and there were no main effects or interactions on time in center of the open field (Fig. 4K- all main effects $p > 0.1$). When anxiety-like behavior was assessed on the elevated zero maze there were no main effects on time in open arms (Fig. 4L all main effects $p > 0.1$), but there was a significant effect of genotype in increasing number of open arm entries (Fig. 4M - $F_{(1,43)} = 9.263$; $p = 0.004$) as well as a main effect of treatment on reducing the number of open arm entries (Fig. 4M $F_{(1,43)} = 6.62$; $p = 0.014$). Interestingly, post-hoc pairwise comparison showed only Wt-Ab/Ac mice displayed a decrease in open arm entries compared to Wt-Abx (Fig. 4M p = 0.019*)*, suggesting that acetate treatment may serve to moderate this anxiety-like behavior as assessed by the elevated zero maze in a microbiome status and genotype dependent manner.

Importantly, serum metabolomics show a main effect of acetate treatment (Supplemental Fig. 2A- $F_{(1,53)} = 4.164$; $p = 0.046$) in increasing serum acetate with minimal other effects on the metabolome (Supplemental Fig 2B–F).

Taken together, these behavioral phenotypes suggest that acetate, which is reduced in *Shank3*^{KO} and further reduced by antibiotics, robustly reverses social deficits caused by *Shank3* genotype, microbiome status, and the interaction. Additionally, acetate supplementation has some more modest effects on microbiome diversity and other behavioral measures including hypolocomotion and anxiety-like behaviors.

3.5 Acetate Replenishment induces unique transcriptional patterns in the mPFC

To identify effects of acetate on central transcriptional regulation, RNA-sequencing on the mPFC was conducted. Here, again all pairwise comparisons made were compared to the ultimate control group (Wt-H_2O) to enable assessment of how each manipulation led to deviations in gene expression from this baseline. Prolonged treatment with Acetate or Ab/Ac resulted in robust changes in gene expression in all groups relative to Wt controls (Fig. 5A–D). Full list of regulated genes from these pairwise comparisons is found in Table S4. Given the ability of oral acetate treatment to rescue *Shank3*^{KO} effects on social behavior, we next examined gene expression patterns between *Shank3*^{KO} and Wt-acetate groups. Here considerable overlap in DGE was found between genotypes (Fig. 5E). Indicating the genes changed by acetate treatment relative to control in each genotype are similar. When the fold change of DGE in each genotype were assessed, symmetry in the direction of gene expression changes is apparent in genes common between the two genotypes (Fig. 5F “Sig. Both”), and genes unique to each genotype (**5F** “Sig. Wt/KO”). Similar patterns of gene overlap and directionality were seen in mice treated with Ab/Ac (Fig. 5G,H).

G:Profiler[51] pathway analysis further revealed treatment with acetate and Ab/Ac resulted in significant regulation of genes involved in metabolic transcription pathways, with a more robust effect in Wt mice (Fig. 5I, bottom and middle – All pathways available in Table S5).

Interestingly, synaptic pathways were generally more enriched in *Shank3*^{KO} mice (Fig. 5I, top). Enrichr analysis of predicted top transcription factors for each pairwise comparison identified numerous activity dependent transcription factors (Creb, Ubtf) and epigenetic regulators (Hdac2) are predicted to be upstream of significant DGE in Acetate and Ab/Ac groups with differential patterns between groups (Fig. 5J).

Given the complexity of our sequencing analysis, we next performed weighted gene coexpression network analysis (WGCNA)[52,53] – a threshold free, data driven approach to identifying multiple genes which are coordinately expressed across genotypes and treatment groups which constitute biologically meaningful changes. Fig. 6A presents a dendrogram module assignment based on gene clustering and Fig. 6B highlights gene modules significantly associated with variables genotype, sex, Abx or Acetate treatment. Abx and acetate treatment were robustly negatively associated with the Purple module (Fig. 6C) which is enriched for processes including nucleic acid binding, and RNA metabolic processing (Fig. 6D). STRING analysis showed a highly interactive network of functional connections between gene products of the purple module, with interconnections far exceeding those predicted by chance Fig. 6E–F. The Brown module was found to be negatively associated with only acetate treatment and is enriched for immune system processes, developmental processes, and response to stress among others (Fig. 6G–J). Interestingly, the GreenYellow module was found to be positively associated with acetate treatment and is enriched for synaptic pathways and cellular localization (Fig. 6K–N). Full pathway analyses from these modules is found in Table S6. Taken together these data demonstrate robust transcriptional effects of acetate in key behaviorally relevant brain regions.

3.6 Levels of Acetate in the serum of patients with Phelan McDermid Syndrome Correlate with ABC Hyperactivity Scores in a Sex Dependent Manner

To assess the relevance of changes in SCFA observed in the *Shank3*^{KO} model to humans, we generated metabolomic data targeting levels of eight SCFAs including acetate across a subset of 32 PMS probands (heterozygous for the *Shank3* gene) and their unaffected controls (Fig.7A). The main sociodemographic and clinical characteristics of study participants are shown in Table S7. Levels of Isobutyric acid and Propionic acid negatively correlated with Vineland communication scores (Fig. 7B). Moreover, sex specific analysis showed levels of acetate negatively correlate with ABC hyperactivity scores in males only (Fig. 7C). A Spearman's correlation confirmed the significant negative correlation ($R = -0.58$ $p<0.05$; Fig. 7D). See Supplemental Results for more detail. Taken together, clinical findings lend further evidence supporting targeting altered levels of SCFAs in PMS patients to improve specific ASD behavioral phenotypes.

(4) Discussion

Here we investigate gene by microbiome interactions in ASD by applying microbiome and metabolite manipulations to a mouse model lacking all isoforms of the *Shank3* gene. *Shank3*^{KO} mice have markedly disrupted gut microbiome composition and function (Fig. 1). *Shank3*^{KO} mice display social deficits and reduced levels of the microbial metabolite

acetate, deficits further exacerbated by antibiotic treatment (Fig. 2). Moreover, mPFC transcriptional responses to Abx treatment were found to be significantly altered by *Shank3* genotype (Fig. 3). Oral treatment with acetate reverses both *Shank3* and microbiome depletion effects on social interaction (Fig. 4), and results in marked transcriptional changes in the mPFC related to synaptic signaling, DNA binding, and metabolism (Fig. 5 and 6). Finally, we verify correlations between levels of acetate and specific behavioral phenotypes in patients with Phelan-McDermid Syndrome – a condition driven by *Shank3* mutations (Fig. 7). These findings highlight acetate as a key mediator of gut-brain signaling in the *Shank3*^{KO} model and provide mechanistic evidence for gene by microbiome interaction in ASD.

A key finding from this study is *Shank3* genotype causes a significant decrease in bacterial diversity and the ratio of Firmicutes and Bacteroidetes. Changes in this ratio are a marker of microbiome dysregulation[54], are associated with behavioral responses to social stress[55] and the production of SCFA metabolites[56]. Our findings are supported by a study utilizing *Shank3* mutant mice lacking the α and β isoforms of *Shank3,* which reported a shift in the ratio of Firmicutes/Bacteroidetes (F/B)[57]. However, while this group found a similar decrease in bacterial diversity, the opposite change in F/B ratio is reported. Similarly, human studies report some patients with ASD present with a decreased Firmicutes/Bacteroidetes ratio[58,59] while others show the opposite result[60,61]. Future studies should closely consider the exact type of genetic mutation associated with an ASD microbiome analysis. We also report that *Lactobacillus* bacteria are decreased in *Shank3*^{KO} mice, consistent with two studies utilizing a model of *Shank3*B deletion[23,24]. These studies noted that supplementation with the *Lactobacillus* species *L. reuteri* rescued social deficits in *Shank3*B knockout mice. Together, our studies highlight specific bacterial groups associated with gut-brain signaling in specific *Shank3* models of ASD.

Using the three-chambered social interaction task, *Shank3* deficient mice were more sensitive to Abx induced social deficits compared to Wt counterparts (Fig. 2G). Global metabolomic analysis of serum further showed KO mice had a more pronounced response to Abx treatment, with 51 significantly altered metabolites compared to 19 in Wt Abx-treated mice which was reversed by acetate treatment (Supp Fig. 2C). Acetate treatment also reversed the decreases in sociability caused by microbiome depletion in both Wt and *Shank3*^{KO} mice and normalized Abx effects on serum metabolic profile (Supp Fig. 2C). These effects of microbiome manipulations on sociability are not surprising and there is growing literature showing microbiome effects on social behaviors[13,41,62]. However these are among the first findings to demonstrate that broad microbiome effects can be reversed via treatment with a single microbiome derived metabolite.

Previous studies have demonstrated alterations to the gut leads to altered gene expression in the brain[15,17,18,63]. Indeed our analysis supports these findings, as RNA sequencing of the mPFC showed transcriptional effects on genes involved in metabolism and nuclear function. These effects were more pronounced in Wt compared to KO mice indicating gene by microbiome interactions on brain transcription. When mice were treated with acetate with or without antibiotics, we found more robust changes in gene expression patterns in the brain (Fig. 5A–D) with convergence in the number of genes that were regulated

in the two genotypes and greater symmetry in the direction of gene expression changes (Fig. 5E–H). WGCNA showed acetate treatment drove robust changes related to immune system processes, cell motility, and synaptic function (Fig. 6). Previous work, largely from the Berger lab, has shown that acetate metabolism can lead to transcriptional regulation and behavioral change in multiple paradigms[49,64,65]. Additionally, acetate can act as a histone deacetylase inhibitor and indirectly influence transcriptional patterns through these mechanisms[48,50].

Finally, examination of the translational relevance of our findings from the *Shank3*^{KO} mouse model revealed no significant genotype effects on levels of acetate in patients with PMS compared to neurotypical controls. However, levels of acetate were found to correlate with ABC hyperactivity scores in male patients (Fig. 6D). Together with our preclinical data, these findings suggest a potential for use of acetate as a biomarker or therapeutic intervention in patients with ASD.

In conclusion, this study shows mice lacking both copies of the *Shank3* display differences in the composition and function of their gut microbiome and are more susceptible to the behavioral metabolic and transcriptional effects of gut microbiome depletion. Importantly, these effects can be reversed by treatment with the gut-derived metabolite acetate independent of microbiome status. These findings provide additional data for a gene by microbiome interaction in the pathophysiology of ASD and carry the potential for bench to bedside translational research in ASD.

Supplementary Material

Refer to Web version on PubMed Central for supplementary material.

Acknowledgements

This work was supported primarily by funds from the Seaver Autism Center and Friedman Brain Institute. A.O. is supported by a Seaver Foundation Fellowship and a NARSAD Young Investigator Award. K.R.M. is supported by NIH grants NS124187 & NS117356. K.L.C. was supported by a postdoctoral fellowship from the Canadian Institutes of Health Research (no. 201811MFE-414896-231226). L.L. is supported by National Institutes of Health (NIH) Medical Scientist Training Program T32 GM07170 and Training Grant in Computational Biology 5-T32-HG-000046-21. We would like to thank Dr. Giulio Pasinetti for thoughtful comments and discussions on the manuscript.

References

1. Volkmar FR, Reichow B & McPartland J. Classification of autism and related conditions: progress, challenges, and opportunities. Dialogues Clin Neurosci 14, 229–237 (2012). [PubMed: 23226949]
2. Satterstrom FK et al. Large-Scale Exome Sequencing Study Implicates Both Developmental and Functional Changes in the Neurobiology of Autism. Cell 180, 568–584.e23 (2020). [PubMed: 31981491]
3. Mila M, Alvarez-Mora MI, Madrigal I. & Rodriguez-Revenga L. Fragile X syndrome: An overview and update of the FMR1 gene. Clin. Genet 93, 197–205 (2018). [PubMed: 28617938]
4. De Rubeis S. et al. Delineation of the genetic and clinical spectrum of Phelan-McDermid syndrome caused by SHANK3 point mutations. Mol Autism 9, 31 (2018). [PubMed: 29719671]
5. Cryan JF & Dinan TG Mind-altering microorganisms: the impact of the gut microbiota on brain and behaviour. Nat Rev Neurosci 13, 701–712 (2012). [PubMed: 22968153]

6. McElhanon BO, McCracken C, Karpen S. & Sharp WG Gastrointestinal symptoms in autism spectrum disorder: a meta-analysis. Pediatrics 133, 872–883 (2014). [PubMed: 24777214]
7. Adams JB, Johansen LJ, Powell LD, Quig D. & Rubin RA Gastrointestinal flora and gastrointestinal status in children with autism--comparisons to typical children and correlation with autism severity. BMC Gastroenterol 11, 22 (2011). [PubMed: 21410934]
8. Ashwood P. et al. Elevated plasma cytokines in autism spectrum disorders provide evidence of immune dysfunction and are associated with impaired behavioral outcome. Brain Behav. Immun 25, 40–45 (2011). [PubMed: 20705131]
9. Macfabe DF Short-chain fatty acid fermentation products of the gut microbiome: implications in autism spectrum disorders. Microb Ecol Health Dis 23, (2012).
10. Ahmed H. et al. Microbiota-derived metabolites as drivers of gut-brain communication. Gut Microbes 14, 2102878 (2022). [PubMed: 35903003]
11. Stilling RM et al. Social interaction-induced activation of RNA splicing in the amygdala of microbiome-deficient mice. Elife 7, (2018).
12. Stilling RM et al. Microbes & neurodevelopment--Absence of microbiota during early life increases activity-related transcriptional pathways in the amygdala. Brain Behav. Immun 50, 209–220 (2015). [PubMed: 26184083]
13. Desbonnet L, Clarke G, Shanahan F, Dinan TG & Cryan JF Microbiota is essential for social development in the mouse. Mol. Psychiatry 19, 146–148 (2014). [PubMed: 23689536]
14. Thion MS et al. Microbiome Influences Prenatal and Adult Microglia in a Sex-Specific Manner. Cell 172, 500–516.e16 (2018). [PubMed: 29275859]
15. Erny D. et al. Host microbiota constantly control maturation and function of microglia in the CNS. Nat. Neurosci 18, 965–977 (2015). [PubMed: 26030851]
16. Kiraly DD et al. Alterations of the Host Microbiome Affect Behavioral Responses to Cocaine. Sci Rep 6, 35455 (2016). [PubMed: 27752130]
17. Hofford RS et al. Alterations in microbiome composition and metabolic byproducts drive behavioral and transcriptional responses to morphine. Neuropsychopharmacology (2021) doi:10.1038/s41386021-01043-0.
18. Chu C. et al. The microbiota regulate neuronal function and fear extinction learning. Nature 574, 543–548 (2019). [PubMed: 31645720]
19. Dohnalová L. et al. A microbiome-dependent gut–brain pathway regulates motivation for exercise. Nature 612, 739–747 (2022). [PubMed: 36517598]
20. Bachmann C, Colombo JP & Berüter J. Short chain fatty acids in plasma and brain: quantitative determination by gas chromatography. Clin Chim Acta 92, 153–159 (1979). [PubMed: 487569]
21. Dalile B, Van Oudenhove L, Vervliet B. & Verbeke K. The role of short-chain fatty acids in microbiota-gut-brain communication. Nat Rev Gastroenterol Hepatol 16, 461–478 (2019). [PubMed: 31123355]
22. James DM et al. Intestinal dysmotility in a zebrafish (Danio rerio) shank3a;shank3b mutant model of autism. Mol Autism 10, 3 (2019). [PubMed: 30733854]
23. Sgritta M. et al. Mechanisms Underlying Microbial-Mediated Changes in Social Behavior in Mouse Models of Autism Spectrum Disorder. Neuron 101, 246–259.e6 (2019). [PubMed: 30522820]
24. Tabouy L. et al. Dysbiosis of microbiome and probiotic treatment in a genetic model of autism spectrum disorders. Brain, Behavior, and Immunity 73, 310–319 (2018). [PubMed: 29787855]
25. Drapeau E, Riad M, Kajiwara Y. & Buxbaum JD Behavioral Phenotyping of an Improved Mouse Model of Phelan-McDermid Syndrome with a Complete Deletion of the Shank3 Gene. eNeuro 5, (2018).
26. Caporaso JG et al. QIIME allows analysis of high-throughput community sequencing data. Nat. Methods 7, 335–336 (2010). [PubMed: 20383131]
27. Clarke EL et al. Sunbeam: an extensible pipeline for analyzing metagenomic sequencing experiments. Microbiome 7, 46 (2019). [PubMed: 30902113]
28. Buchfink B, Xie C. & Huson DH Fast and sensitive protein alignment using DIAMOND. Nat Methods 12, 59–60 (2015). [PubMed: 25402007]

29. Kanehisa M. & Goto S. KEGG: kyoto encyclopedia of genes and genomes. Nucleic Acids Res 28, 27–30 (2000). [PubMed: 10592173]
30. Love MI, Huber W. & Anders S. Moderated estimation of fold change and dispersion for RNA-seq data with DESeq2. Genome Biol 15, 550 (2014). [PubMed: 25516281]
31. Ritchie ME et al. limma powers differential expression analyses for RNA-sequencing and microarray studies. Nucleic Acids Res. 43, e47 (2015). [PubMed: 25605792]
32. Leek JT, Johnson WE, Parker HS, Jaffe AE & Storey JD The sva package for removing batch effects and other unwanted variation in high-throughput experiments. Bioinformatics 28, 882–883 (2012). [PubMed: 22257669]
33. Kuleshov MV et al. Enrichr: a comprehensive gene set enrichment analysis web server 2016 update. Nucleic Acids Research 44, W90–W97 (2016). [PubMed: 27141961]
34. Zhao S, Li H, Han W, Chan W. & Li L. Metabolomic Coverage of Chemical-Group-Submetabolome Analysis: Group Classification and Four-Channel Chemical Isotope Labeling LC-MS. Anal. Chem 91, 12108–12115 (2019). [PubMed: 31441644]
35. Breen MS et al. Large 22q13.3 deletions perturb peripheral transcriptomic and metabolomic profiles in Phelan-McDermid syndrome. Human Genetics and Genomics Advances 4, 100145 (2023). [PubMed: 36276299]
36. Hills RD et al. Gut Microbiome: Profound Implications for Diet and Disease. Nutrients 11, (2019).
37. Fields CT et al. Defining Dysbiosis in Disorders of Movement and Motivation. J. Neurosci 38, 9414–9422 (2018). [PubMed: 30381433]
38. van Sadelhoff JHJ et al. The Gut-Immune-Brain Axis in Autism Spectrum Disorders; A Focus on Amino Acids. Front Endocrinol (Lausanne) 10, 247 (2019). [PubMed: 31057483]
39. Dinan TG & Cryan JF The Microbiome-Gut-Brain Axis in Health and Disease. Gastroenterol. Clin. North Am 46, 77–89 (2017). [PubMed: 28164854]
40. Levy DR et al. Dynamics of social representation in the mouse prefrontal cortex. Nat Neurosci 22, 2013–2022 (2019). [PubMed: 31768051]
41. Sherwin E, Bordenstein SR, Quinn JL, Dinan TG & Cryan JF Microbiota and the social brain. Science 366, (2019).
42. Fortier AV, Meisner OC, Nair AR & Chang SWC Prefrontal circuits guiding social preference: Implications in autism spectrum disorder. Neurosci Biobehav Rev 141, 104803 (2022). [PubMed: 35908593]
43. Pagani M. et al. Deletion of Autism Risk Gene Shank3 Disrupts Prefrontal Connectivity. J Neurosci 39, 5299–5310 (2019). [PubMed: 31061091]
44. Yoo T, Yoo Y-E, Kang H. & Kim E. Age, brain region, and gene dosage-differential transcriptomic changes in Shank3-mutant mice. Front Mol Neurosci 15, 1017512 (2022). [PubMed: 36311023]
45. Jacot-Descombes S. et al. Altered synaptic ultrastructure in the prefrontal cortex of Shank3-deficient rats. Mol Autism 11, 89 (2020). [PubMed: 33203459]
46. Gacias M. et al. Microbiota-driven transcriptional changes in prefrontal cortex override genetic differences in social behavior. Elife 5, (2016).
47. Hoban AE et al. Regulation of prefrontal cortex myelination by the microbiota. Transl Psychiatry 6, e774 (2016). [PubMed: 27045844]
48. Soliman ML & Rosenberger TA Acetate supplementation increases brain histone acetylation and inhibits histone deacetylase activity and expression. Mol Cell Biochem 352, 173–180 (2011). [PubMed: 21359531]
49. Mews P. et al. Alcohol metabolism contributes to brain histone acetylation. Nature 574, 717–721 (2019). [PubMed: 31645761]
50. Frost G. et al. The short-chain fatty acid acetate reduces appetite via a central homeostatic mechanism. Nat Commun 5, 3611 (2014). [PubMed: 24781306]
51. Raudvere U. et al. g:Profiler: a web server for functional enrichment analysis and conversions of gene lists (2019 update). Nucleic Acids Res. 47, W191–W198 (2019). [PubMed: 31066453]
52. Langfelder P. & Horvath S. WGCNA: an R package for weighted correlation network analysis. BMC Bioinformatics 9, 559 (2008). [PubMed: 19114008]

53. Sens JP, Hofford RS & Kiraly DD Effect of germ-free status on transcriptional profiles in the nucleus accumbens and transcriptomic response to chronic morphine. Mol Cell Neurosci 103874 (2023) doi:10.1016/j.mcn.2023.103874.

54. Iannone LF et al. Microbiota-gut brain axis involvement in neuropsychiatric disorders. Expert Rev Neurother 19, 1037–1050 (2019). [PubMed: 31260640]

55. Partrick KA et al. Acute and repeated exposure to social stress reduces gut microbiota diversity in Syrian hamsters. Behavioural Brain Research 345, 39–48 (2018). [PubMed: 29474810]

56. Machiels K. et al. A decrease of the butyrate-producing species Roseburia hominis and Faecalibacterium prausnitzii defines dysbiosis in patients with ulcerative colitis. Gut 63, 1275–1283 (2014). [PubMed: 24021287]

57. Sauer AK, Bockmann J, Steinestel K, Boeckers TM & Grabrucker AM Altered Intestinal Morphology and Microbiota Composition in the Autism Spectrum Disorders Associated SHANK3 Mouse Model. International Journal of Molecular Sciences 20, 2134 (2019). [PubMed: 31052177]

58. De Angelis M. et al. Fecal microbiota and metabolome of children with autism and pervasive developmental disorder not otherwise specified. PLoS ONE 8, e76993 (2013). [PubMed: 24130822]

59. Zhang M, Ma W, Zhang J, He Y. & Wang J. Analysis of gut microbiota profiles and microbe-disease associations in children with autism spectrum disorders in China. Sci Rep 8, 13981 (2018). [PubMed: 30228282]

60. Strati F. et al. New evidences on the altered gut microbiota in autism spectrum disorders. Microbiome 5, 24 (2017). [PubMed: 28222761]

61. Tomova A. et al. Gastrointestinal microbiota in children with autism in Slovakia. Physiology & Behavior 138, 179–187 (2015). [PubMed: 25446201]

62. Desbonnet L. et al. Gut microbiota depletion from early adolescence in mice: Implications for brain and behaviour. Brain Behav. Immun 48, 165–173 (2015). [PubMed: 25866195]

63. Hoban AE et al. The microbiome regulates amygdala-dependent fear recall. Mol. Psychiatry 23, 1134–1144 (2018). [PubMed: 28507320]

64. Alexander DC et al. Targeting acetyl-CoA metabolism attenuates the formation of fear memories through reduced activity-dependent histone acetylation. Proceedings of the National Academy of Sciences 119, e2114758119 (2022).

65. Mews P. et al. Acetyl-CoA synthetase regulates histone acetylation and hippocampal memory. Nature 546, 381–386 (2017). [PubMed: 28562591]

Highlights

- Shank3^{KO} mice have decreased microbiome diversity and decreased social preference. Depletion of the microbiome further decreases social preference.
- Levels of the microbiome derived metabolite acetate are decreased in Shank3^{KO} mice and are further decreased by antibiotic depletion of the microbiome.
- Supplementation of acetate via the drinking water reverses social deficits in Shank3^{KO} mice, both in those with an intact microbiome and those with a depleted microbiome.
- Acetate induces unique transcriptional patterns in the medial prefrontal cortex affecting gene expression related to synaptic plasticity and immune function.
- Patients with Phelan McDermid Syndrome, who carry mutations to the Shank3 gene, exhibit correlations of acetate with clinical hyperactivity scores.

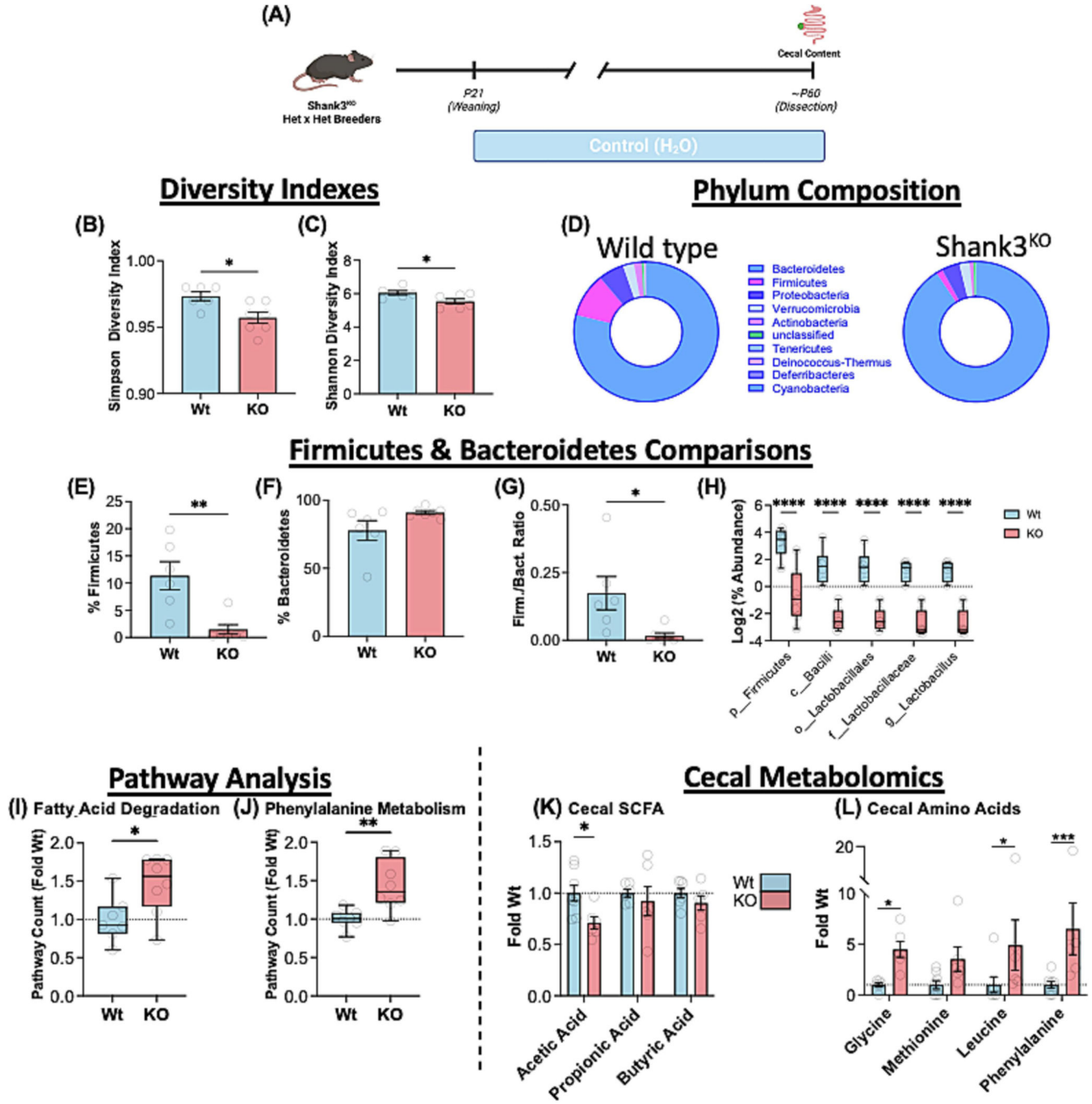

Figure 1: Deletion of the *Shank3* Gene Results in a Dysregulated Gut Microbiome and Metabolome

(A) Study design for experiment 1 and cecal content collection. Shank3 ^{KO} mice show decreased microbiome diversity by Simpson. **(B)** and Shannon. **(C)** diversity metrics. **(D)** Donut charts showing the relative Phylum composition of Wt and *Shank3*^{KO} mice. **(E)** Relative composition of bacteria from the Firmicutes phylum was decreased in *Shank3*^{KO}. **(F)** but no significant difference in Bacteroidetes. **(G)** The ratio of Firmicutes to Bacteroidetes is significantly decreased in Shank3^{KO} mice. **(H)** Relative abundance of

phylogenies containing *Lactobacillus* showed decreases across all taxonomic levels, n = 6–7 mice per genotype for 16S analysis. **(I)** Functional KEGG pathway counts for Fatty Acid degradation and **(J)** Phenylalanine metabolism were both significantly increased in *Shank3*^{KO} mice, n = 7–8 mice per genotype for Shotgun metagenomic analysis. **(K)** Targeted metabolomics shows levels of Short Chain Fatty Acid (SCFA) Acetic Acid are significantly decreased in *Shank3*^{KO} mice. **(L)** Levels of amino acid Phenylalanine were significantly increased in Shank3^{KO} mice. n = 6–8 mice per group for cecal targeted metabolomic analysis. All data presented as mean ± SEM *p<0.05 **p<0.01 ***p<0.001. Male and female mice were used in all analysis.

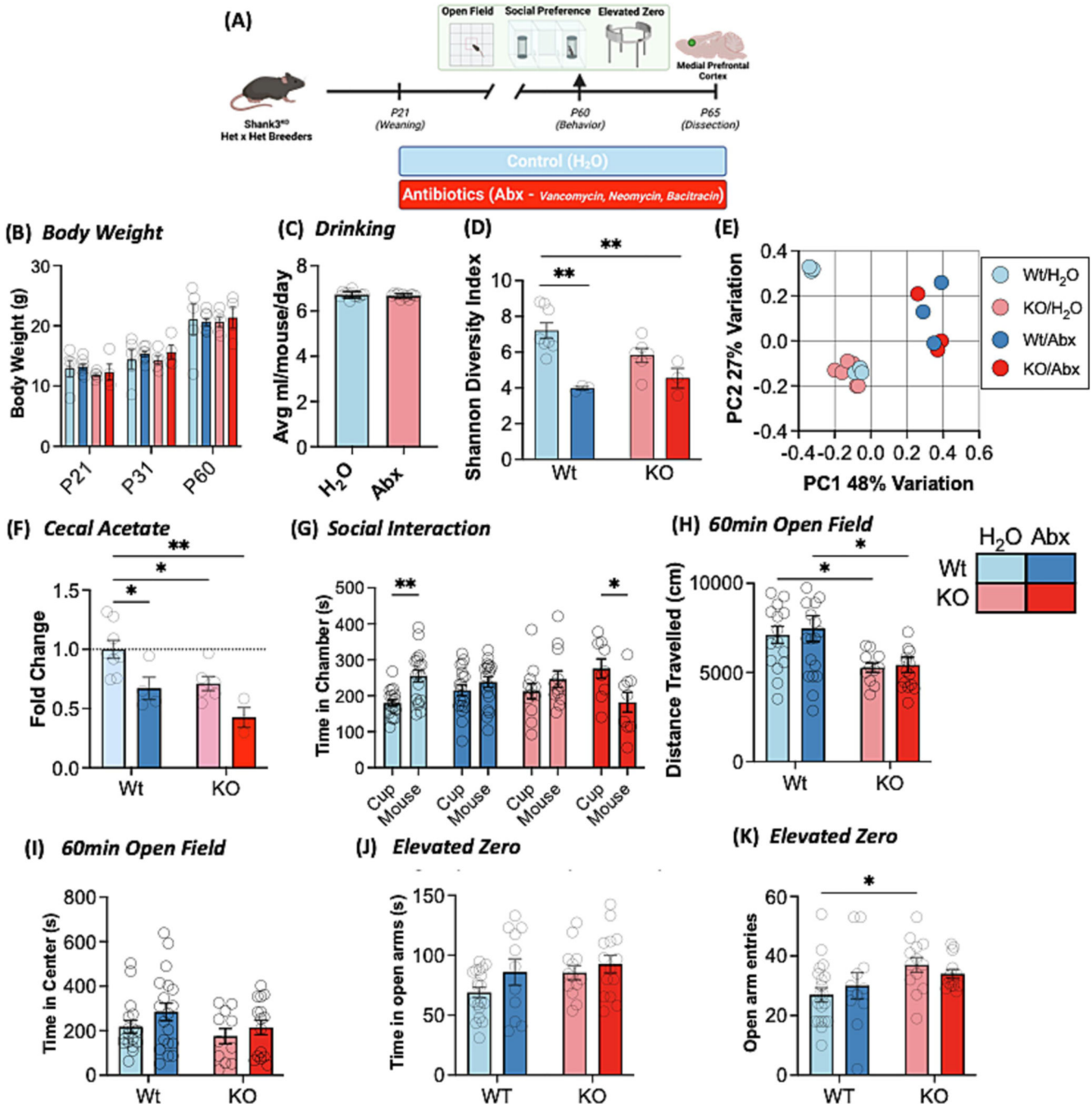

Figure 2: Antibiotic Treatment Throughout Development Exacerbates Metabolic and Social Deficits Caused by *Shank3* Deletion

(A) Study design for Experiment 2 and mPFC collection. **(B)** Wild-type and Shank*3*^{KO} mice show normal body weight growth over time regardless of genotype or treatment n = 4–7 mice per genotype for weight gain analysis. **(C)** mice of both genotypes drink the same amount of control or Abx treated water; n = 12 mice per treatment group. **(D)** Antibiotics result in marked depletion of microbial diversity in both Wt and *Shank3*^{KO} mice by Shannon diversity index. **(E)** Unweighted PCOA plot of beta diversity shows a marked shift induced

by antibiotic treatment in both genotypes. **(F)** Levels of Acetic Acid were decreased in control Shank3^{KO} mice and further decreased by Abx treatment n = 3– 8 mice for both 16S and targeted metabolomic analysis. **(G)** In the three-chambered social interaction task, Wt-H_2O mice spent increased time in the chamber containing the novel social interactor while *Shank3*^{KO}-H_2O did not show a significant preference for the social interactor. Treatment with Abx caused Wt mice to lose social preference and exacerbated social deficits in KO mice, n = 9–19 mice per genotype and treatmen.t **(H)** *Shank3*^{KO} mice show decreased locomotion in 60-minute open field not affected by antibiotics. **(I)** No genotype or treatment differences are seen on time in center of an open field, n = 12–19 mice per genotype and treatment for open field. **(J)** In the elevated O-maze no significant differences in total time spent in the open arms is found. **(K)** *Shank3*^{KO}-H_2O mice display increased frequency of entries into the open arm of the elevated zero maze, n = 11–19 mice per genotype and treatment. All data presented as mean ± SEM. *$p < 0.05$; **$p < 0.01$; ***$p < 0.001$; ****$p < 0.0001$. Male and female mice were used for all analysis.

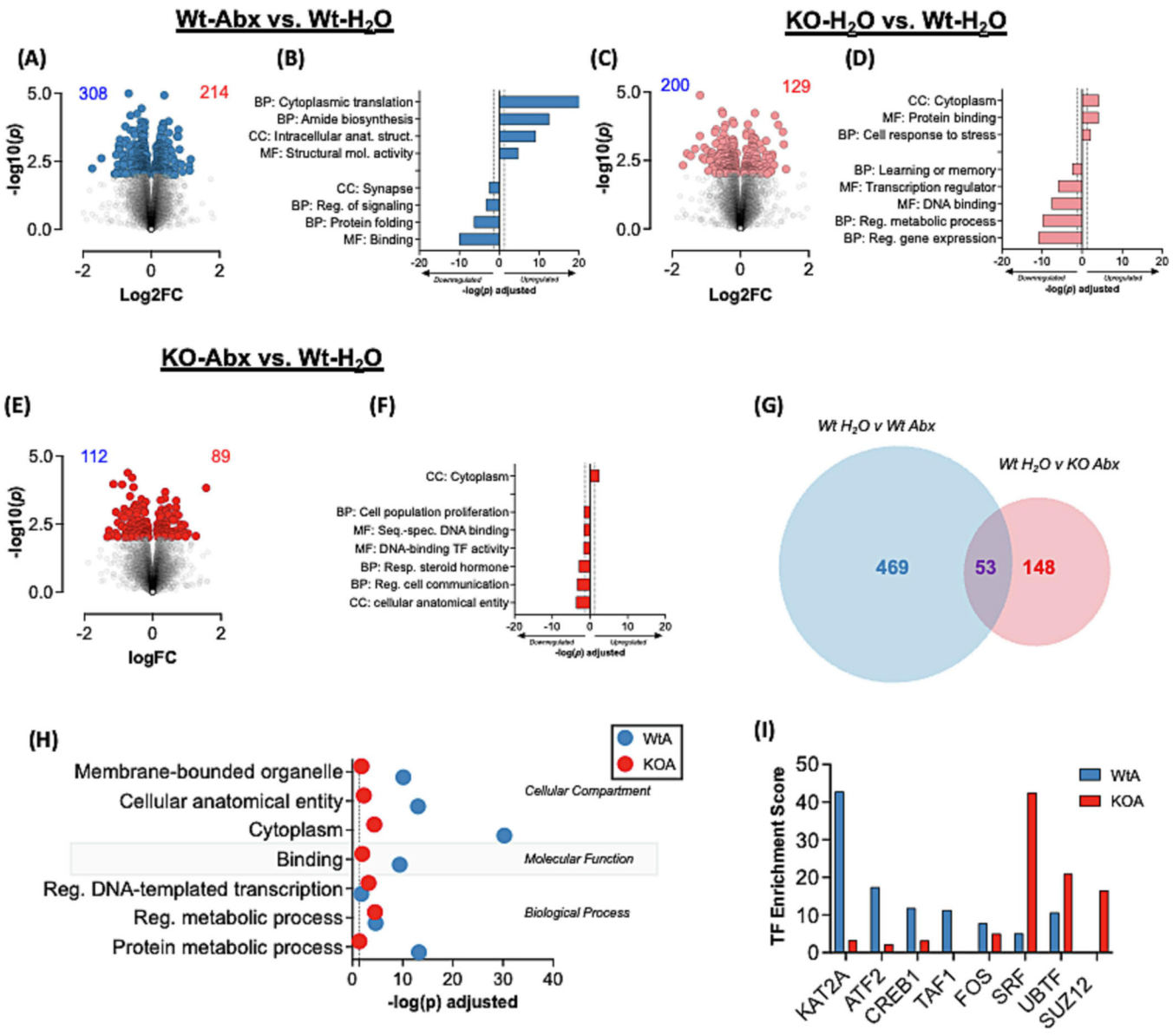

Figure 3: Effects of *Shank3* Deletion and Antibiotic Treatment on mPFC Gene Expression.

(A) Volcano plot of gene expression changes comparing Wt-H_2O and Wt-Abx. **(B)** Select gene pathways regulated in Abx treated Wt mice. Dotted line at 1.3 indicates significance (FDR corrected $p<0.05$). **(C)** Volcano plot of gene expression changes comparing Wt-H_2O and *Shank3*^{KO}-H_2O mice. **(D)** Select pathways that are predicted to be regulated in *Shank3*^{KO} mice. **(E)** Volcano plot of gene expression changes comparing KO-H_2O and KO-Abx. **(F)** Select pathways that are predicted to be regulated in KO-Abx mice. **(G)** Venn diagram of all significant genes in Wt-Abx and KO-Abx relative to Wt-H_2O controls shows the two genotypes have highly disparate responses to prolonged microbiome depletion. **(H)** Gene ontology analysis of regulated genes in Wt and KO mice following Abx. **(I)** Top Transcription Factors (TF) predicted to be upstream from differentially expressed genes in Wt-Abx and KO-Abx groups relative to Wt-H_2O controls. n = 3–6 mice per genotype and treatment group. Male and female mice were used for all analysis

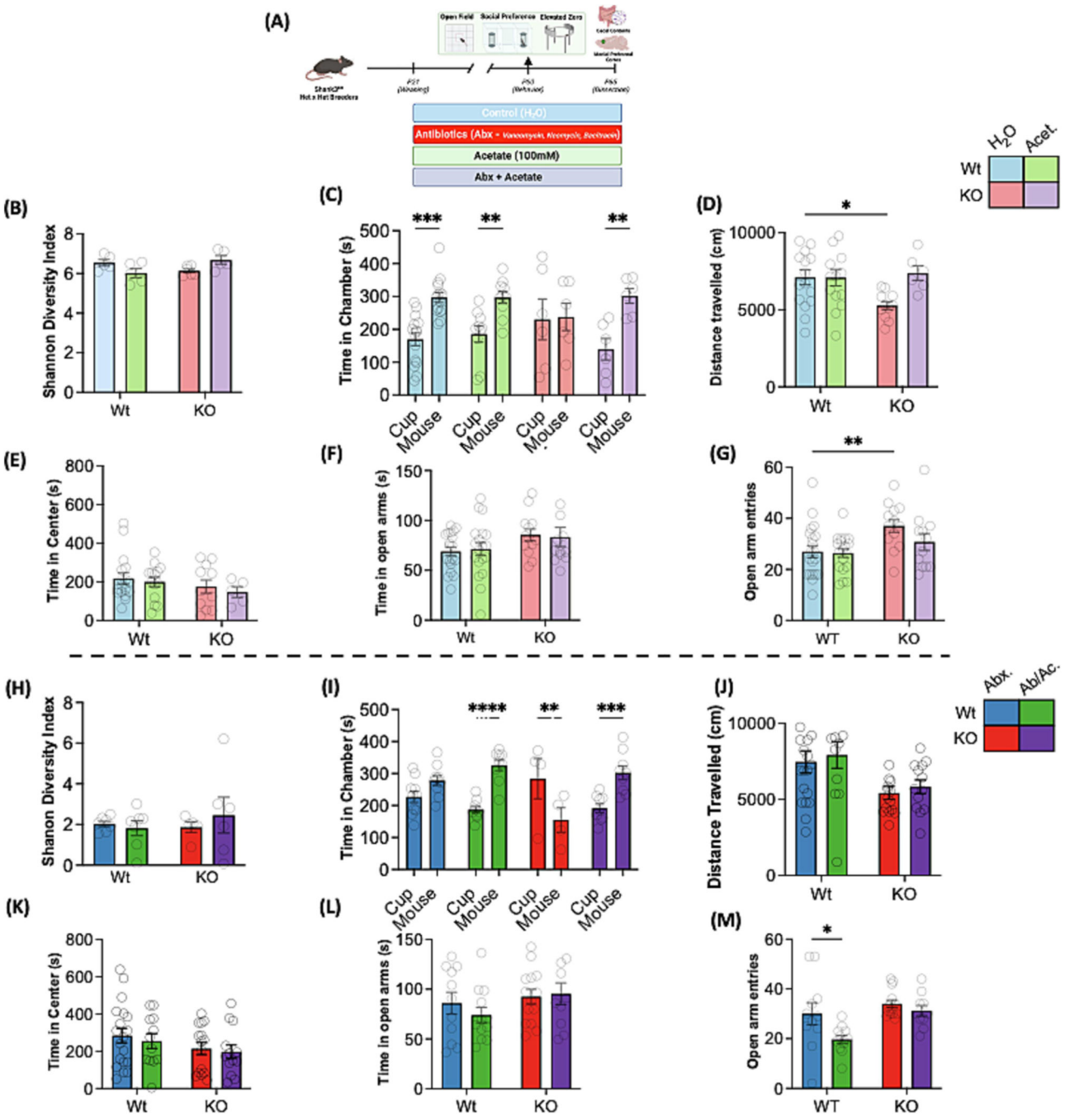

Figure 4: Acetate Replenishment Rescues Social Deficits Caused by Shank3 Deletion Independent of an Intact Microbiome

(A) Study design for Experiment 3 and mPFC collection. **(B)** Acetate treatment interacts with genotype to slightly alter microbiome diversity by Shannon diversity index. $n = 6–7$ mice per group for 16S analysis. **(C)** In the three-chambered social interaction task, Wt-H_2O and Wt-Acetate mice spent increased time in the chamber containing the novel social interactor (blue and green bars). Shank3^{KO}-H_2O did not show a significant preference for the social interactor at baseline as previous (pink bars). Acetate treatment rescues this social

deficit in Shank3^{KO} mice (purple bars). n = 6–15 mice per genotype and treatment. **(D)** Acetate treatment also reverses locomotor activity deficit in Shank3^{KO} in a 60 minute open field task. **(E)** No genotype or treatment effects on time spent in center of open field in a 60 minute test session. n = 6–16 mice per genotype and treatment for open field. **(F)** *Shank3*^{KO} control and acetate treated spend more time spent in open arms of elevated zero maze. **(G)** *Shank3* ^{KO}-H_2O mice display increased frequency of entries into the open arm, but not those treated with acetate n = 12–20 mice per genotype and treatment for zero maze. **(H)** Treatment with acetate does not reverse Abx effects on microbiome diversity by Shannon diversity index. n = 6–7 mice per group for 16S analysis. **(I)** In the three-chambered social interaction task, Wt-Abx mice do not show a significant preference for the novel social interactor (blue bars). Treatment with acetate in microbiome depleted (Ab/Ac) mice reverse this phenotype (green bars). Shank3 ^{KO}-Abx mice again demonstrate an aversion for the social stimulus (red bars), but this is reversed when acetate is supplemented to the antibiotics (Ab/Ac – purple bars). n = 4–10 mice per genotype and treatment for 3 chamber. **(J)** Abx or Ab/Ac do not alter Shank3 genotype effects on locomotion in a 1-hour open field test session. **(K)** No genotype or treatment effects on time spent in center of open field in a 60-minute test session. n = 12–19 mice per genotype and treatment for open field. **(L)** Treatment with Abx or Ab/Ac does not alter Shank3 genotype effects on time spent in open arms of the o-maze. **(M)** Wt Ab/Ac mice display decreased frequency of entries into the open arm of the elevated zero maze compared to Wt-Abx mice. n = 10–14 mice per genotype and treatment for zero maze. All data presented as mean ± SEM. *$p < 0.05$; **$p < 0.01$; ***$p < 0.001$; ****$p < 0.0001$. Male and female mice were used in all analysis.

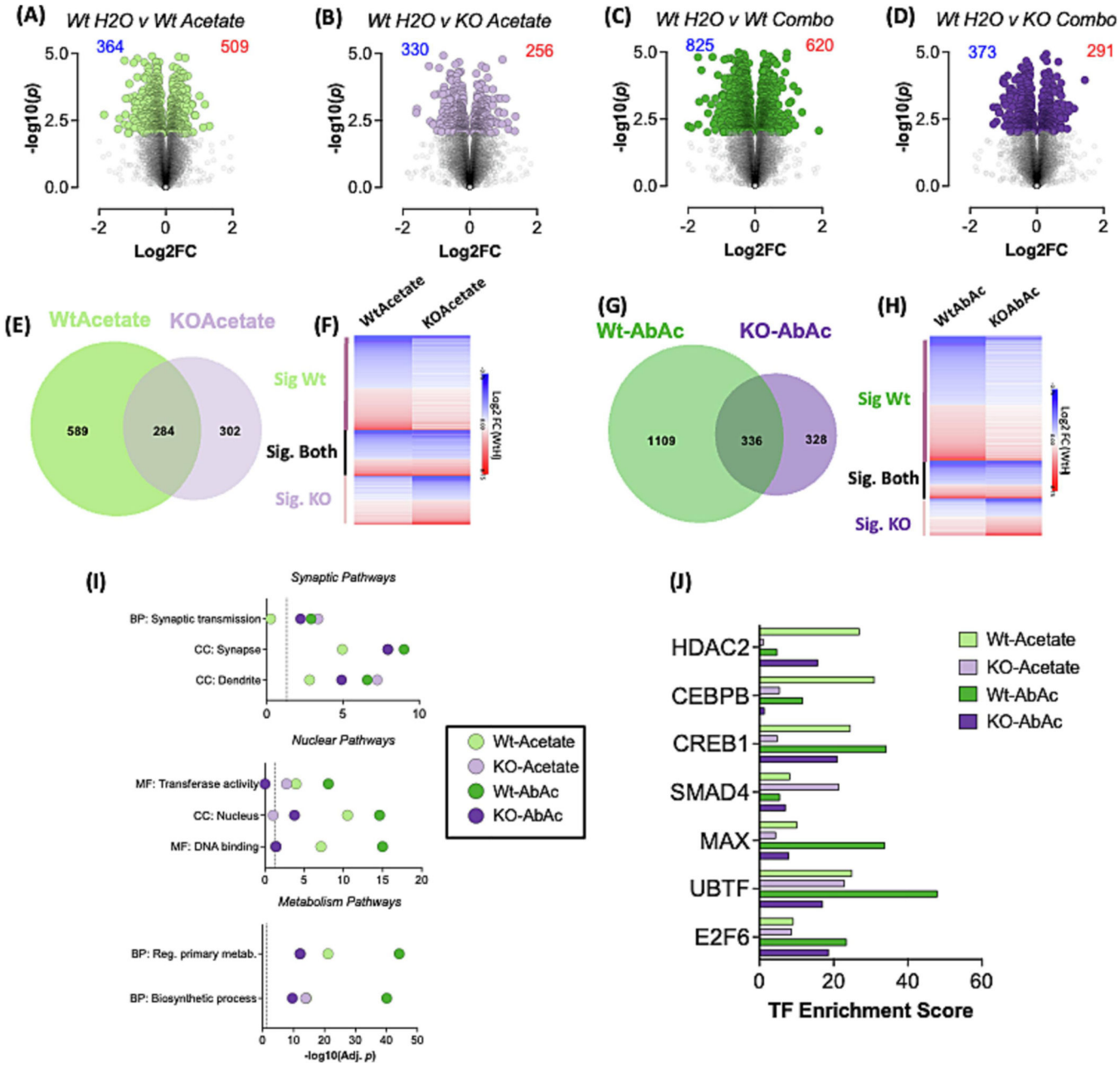

Figure 5: Treatment with acetate induces unique transcriptional patterns in the mPFC

(A-D) Volcano plots of all Acetate and Ab/Ac treatment groups relative to Wt-H_2O controls. **(E)** Venn diagram of all genes significantly regulated in Wt-Acetate and KO-Acetate relative to Wt-H_2O. **(F)** Heatmap of fold change expression of all genes from the previous panel **(G)** Venn diagram of all genes significantly regulated in Wt-Ab/Ac and KO-Ab/Ac relative to Wt-H_2O. **(H)** Heatmap of fold change expression of all genes from the previous panel **(I)** Select pathways predicted to be enriched in uniquely regulated genes in Wt and KO mice from the four treatment groups. **(J)** Transcription factors predicted to be upstream of significantly regulated genes relative to Wt-H_2O controls. n = 4–6 mice per genotype and treatment group. Male and female mice were used for all analysis.

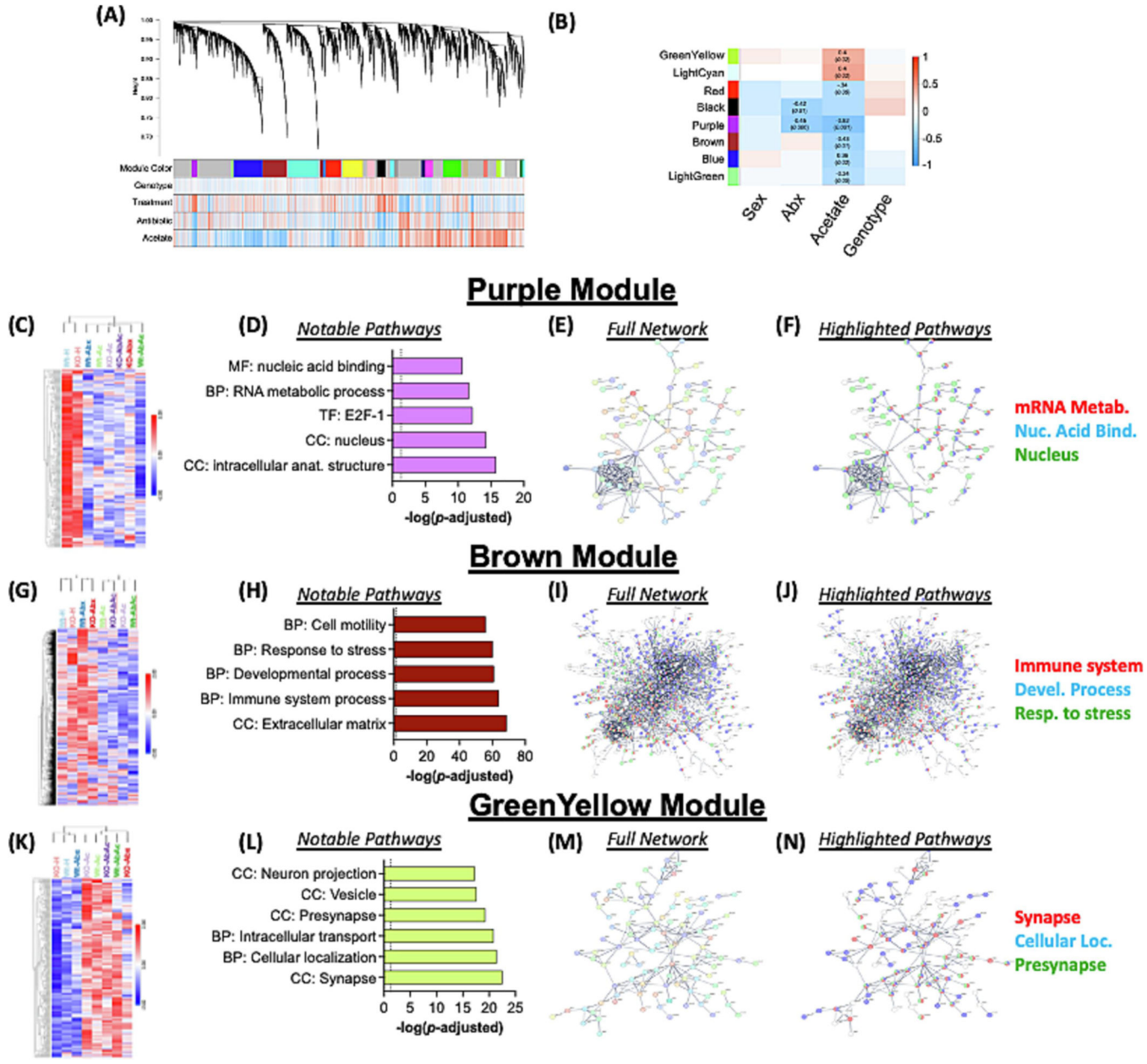

Figure 6: Weighted Gene Network Analysis Reveals Acetate Treatment Alters Transcription of Genes involved in metabolism, Immune system and Synpatic Function

(A) Dendrogram of WGCNA analysis. **(B)** Module-trait relationship table showing modules of interest. Each cell reports the Pearson correlation value and if significant the *p*-value in parentheses. Columns describe the variable, and the rows show the module name **(C)** Heatmap showing unsupervised hierarchical clustering of all genes in Purple module. **(D)** Gene ontology enrichment of the differentially expressed genes in Purple module. **(E)** Protein-protein interaction (PPI) network enrichment for the Purple module from the STRING database. **(F)** Select pathways from full PPI network enrichment for the purple module from STRING database. **(G-J)** Heatmap, gene ontology enrichment and PPI network enrichment for genes in Brown module. **(K-N)** Heatmap, gene ontology enrichment

and PPI network enrichment for genes in Green Yellow module. n = 4–6 mice per group. Male and female mice were used for all analysis.

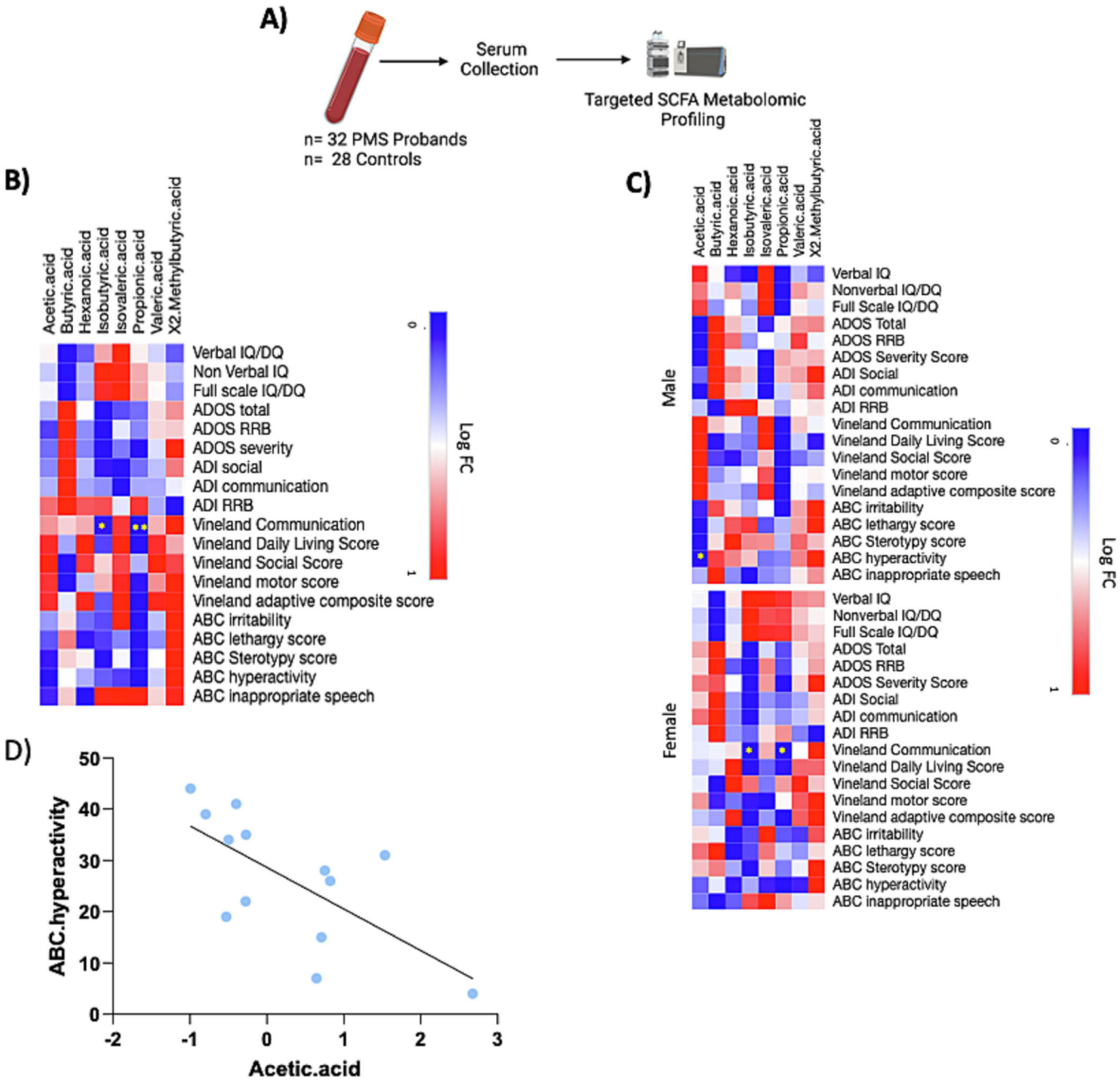

Figure 7: Serum Levels of Acetate Correlate with ABC Hyperactivity in Male PMS Patients

(A) Study Design: Clinical scores as well as serum was collected from 32 PMS probands and 28 unaffected family controls. Serum was then analyzed for levels of 8 SCFAs using liquid chromatography-mass spectrometry (LC/MS) (**B**) Heatmap showing a significant correlation between Vineland Communication scores and levels of Isobutyric acid and propanoic acid n =30) (**C**) Heatmap showing a significant negative correlation between Vineland Communication scores and levels of Isobutyric acid and propanoic acid in females only (n =17) and significant negative correlation between ABC hyperactivity scores and Acetic Acid levels in males (n= 13) **(D)** Spearman's correlation confirming significant

negative correlation between levels of acetic acid and ABC hyperactivity in males (R= −0.5824). *$p < 0.05$; **$p < 0.01$